Prepared for submission to JINST

4TH European Conference on Plasma Diagnostics
7–11 June 2021
Salamanca, Spain

Inference of molecular divertor density from filtered camera analysis of molecularly induced Balmer line emission during detachment in JET L-mode plasmas

J. Karhunen,[a,1] **A. Holm,**[b] **B. Lomanowski,**[c] **V. Solokha,**[b] **S. Aleiferis,**[d] **P. Carvalho,**[e] **M. Groth,**[b] **K.D. Lawson,**[f] **A.G. Meigs,**[f] **A. Shaw**[f] **and JET Contributors**[2]

[a] *Department of Physics, University of Helsinki, Helsinki, Finland*
[b] *Aalto University, Department of Applied Physics, Espoo, Finland*
[c] *Oak Ridge National Laboratory, Oak Ridge, TN, USA*
[d] *Institute of Nuclear and Radiological Sciences and Technology, Energy and Safety; National Centre for Scientific Research 'Demokritos', Athens, Greece*
[e] *Instituto de Plasmas e Fusão Nuclear, Instituto Superior Técnico, Lisboa, Portugal*
[f] *CCFE, Culham Science Centre, Abingdon, UK*

E-mail: juuso.karhunen@ukaea.uk

Abstract: A previously presented Monte Carlo method for estimating local plasma conditions in 2D based on intensity ratios of deuterium Balmer D_α, D_γ and D_ε lines was amended to consider also the D_α and D_γ emission contributions arising from molecular processes. The obtained estimates was used to infer the molecular divertor density with the help of the molecular databases of EIRENE. The method was benchmarked against EDGE2D-EIRENE simulations and observed to reproduce the molecularly induced emission fractions and the molecular divertor densities primarily within 25% of the references. Experimental analysis of a JET L-mode density scan suggested molecularly induced D_α and D_γ contributions of up to 60–70% and 20%, respectively, during the process of detachment. The independent estimates inferred from the obtained molecularly induced D_α and $D\gamma$ intensities agree within uncertainties on the molecular divertor density increasing up to approximately 3.0×10^{20} m^{-3} at the outer strike point in deep detachment with its ratio to the local electron density agreeing with EDGE2D-EIRENE predictions within the scatter of the experimental data.

Keywords: Nuclear instruments and methods for hot plasma diagnostics; Plasma diagnostics – interferometry, spectroscopy and imaging; Plasma diagnostics – high speed photography

[1] Corresponding author.

[2] See the author list of "Overview of the JET results for optimising ITER operation" by J. Mailloux et al. to be published in Nuclear Fusion Special issue: Overview and Summary Papers from the 28th Fusion Energy Conference (Nice, France, 10–15 May 2021)

Contents

1 Introduction

Measurements of the deuterium Balmer line emission provide essential reference data for divertor plasma modelling via direct comparison of measured and simulated line intensities or by post-processing the emission measurements to yield information on the different divertor plasma parameters. The interpretation of the emission with the help of traditional atomic data is, however, interfered by molecular processes in the plasma, which lead to excitation of D atoms via reactions involving D_2, D_2^+, D_3^+ and D^-, resulting in an additional Balmer emission contribution [1, 2]. This molecularly induced emission component has previously been observed to potentially even dominate the Balmer D_α intensity at the onset of detachment [2, 3].

In this work, a Monte Carlo method previously presented in [4, 5] for estimating local divertor plasma conditions from filtered camera observations of Balmer emission has been amended to distinguish the molecularly induced contributions from the total emission intensities. The separated emission contributions have been further post-processed to provide estimates of the molecular divertor density. The method has been benchmarked with the help of EGDE2D-EIRENE [6–8] simulations and demonstrated experimentally during detachment in a JET L-mode density scan.

2 Inferring molecularly induced Balmer emission contribution and molecular divertor density

2.1 Estimating molecularly induced D_α and D_γ emission

Methodology for local 2D estimates of the electron density, n_e, electron temperature, T_e, and atomic density, n_{at}, in the JET divertor volume was introduced in [4, 5], based on intensity ratios of reflection-corrected tomographic reconstructions [9–12] of divertor camera images of the

Balmer D_α, D_γ and D_ε emissions. The estimates are provided as results of a Markov Chain Monte Carlo [13, 14] optimization model with the help of atomic data of the ADAS database [15] and constraints from line-integrated spectroscopic measurements of the divertort n_e and T_e [16–18]. The ADAS representation, however, considers only emission arising from purely atomic processes as a sum of electron-impact excitation and recombination, ignoring thus the additional contribution from molecular processes.

The method presented in [4, 5] has been amended to consider molecular processes by treating the emission intensity, $I_{p\to q}$, of a given electronic transition between principal quantum states p and q as a sum of its purely atomic and molecularly induced components:

$$I_{p\to q} = I_{p\to q,at} + I_{p\to q,mol}. \tag{2.1}$$

By expanding the purely atomic component with its ADAS representation and considering the molecularly induced component as a fraction f_{mol} of the total intensity, $I_{p\to q}$ can be presented as

$$\begin{aligned} I_{p\to q} &= \underbrace{\frac{1}{4\pi}\left[\overbrace{n_{at}n_e PEC^{exc}_{p\to q}(n_e,T_e)}^{\text{excitation}} + \overbrace{n_i n_e PEC^{rec}_{p\to q}(n_e,T_e)}^{\text{recombination}}\right]}_{\text{atomic}} + \underbrace{f_{mol} I_{p\to q}}_{\text{molecular}} \\ &\approx \frac{1}{4\pi\,(1-f_{mol})}\left[n_{at}n_e PEC^{exc}_{p\to q}(n_e,T_e) + n_e^2 PEC^{rec}_{p\to q}(n_e,T_e)\right]. \end{aligned} \tag{2.2}$$

Here, $PEC^{exc/rec}_{p\to q}(n_e,T_e)$ are the n_e- and T_e-dependent ADAS photon emission coefficients for electron-impact excitation and recombination processes, and a simplification of equal ion and electron densities, $n_i \approx n_e$, has been made, as discussed in [5].

The molecularly induced contributions of the D_α and D_γ emissions, $f_{mol,\alpha}$ and $f_{mol,\gamma}$, have been introduced as new variables in the optimization model of [4, 5] by replacing the purely atomic representation of the emission with the formalism of equation (2.2). Consequently, the amended model provides 2D estimates for n_e, T_e, n_{at}, $f_{mol,\alpha}$ and $f_{mol,\gamma}$. The increase in the unknown variables is facilitated by using a solution of the optimization model without the molecularly induced contributions as the initial state for the amended model with $f_{mol,\alpha}$ and $f_{mol,\gamma}$ included and tightening the line-integrated constraints for n_e and T_e. No constraints are set for $f_{mol,\alpha}$ and $f_{mol,\gamma}$, but they are allowed to range freely between 0.0 and 0.99 with no coupling to the other plasma parameters via any physical predictions. To avoid a further increase of the unknown variables, D_ε emission is assumed to be relatively free of the molecularly induced contribution. In lack of direct reference data for D_ε, this is supported by the general trend of decreasing effect of the molecular processes on the total intensity with increasing excitation state and the low molecularly induced contributions observed for the D_δ line synthetically in preparation for this work and experimentally at TCV [2].

2.2 Inferring molecular density from molecularly induced emission

The AMJUEL and H2VIBR atomic and molecular databases of EIRENE provide means for calculating the molecularly induced Balmer emission contributions for H_α, H_β, H_γ and H_δ according to

$$I_{p\to q,mol} = \frac{1}{4\pi}\sum_{H^\star}\sum_{\nu} A_{p\to q} n_{mol} f_\nu(T_e)\, N^{H^\star\to H(p)}_{H(p)/H^\star}(n_e,T_e)\, R^{H_2(\nu)\to H^\star}_{H^\star/H_2}(n_e,T_e,\nu), \tag{2.3}$$

where $A_{\mathrm{p}\to\mathrm{q}}$ is the Einstein coefficient for spontaneous emission in the given electronic transition. $N^{\mathrm{H}^\star\to\mathrm{H(p)}}_{\mathrm{H(p)/H}^\star}(n_\mathrm{e},T_\mathrm{e})$ and $R^{\mathrm{H}_2(\nu)\to\mathrm{H}^\star}_{\mathrm{H}^\star/\mathrm{H}_2}(n_\mathrm{e},T_\mathrm{e},\nu)$ describe the population of H atoms at excitation state p arising from processes involving molecular species $\mathrm{H}^\star$ and the generation of $\mathrm{H}^\star$ from H_2 molecules, respectively, and are obtained as ratios to the $\mathrm{H}^\star$ and H_2 densities from AMJUEL and H2VIBR. Both are functions of n_e and T_e, while the latter also depends on the vibrational excitation state, ν, of the H_2 molecules, whose fractional abundance is given by the scaling factor $f_\nu(T_\mathrm{e})$. If the molecularly induced emission contributions are successfully distinguished with methods described above, and they are assumed to arise from processes involving H_2, H_2^+, H_3^+ and H^-, as discussed in [1], an estimate for the molecular divertor density can be derived from equation (2.3) as

$$n_\mathrm{mol} = \frac{4\pi I_{\mathrm{p}\to\mathrm{q,mol}}}{A_{\mathrm{p}\to\mathrm{q}}\sum_\nu f_\nu\left[N^{\mathrm{H}_2\to\mathrm{H(p)}}_{\mathrm{H(p)/H}_2} + N^{\mathrm{H}_2^+\to\mathrm{H(p)}}_{\mathrm{H(p)/H}_2^+} R^{\mathrm{H}_2(\nu)\to\mathrm{H}_2^+}_{\mathrm{H}_2^+/\mathrm{H}_2} + N^{\mathrm{H}_3^+\to\mathrm{H(p)}}_{\mathrm{H(p)/H}_3^+} R^{\mathrm{H}_2(\nu)\to\mathrm{H}_3^+}_{\mathrm{H}_3^+/\mathrm{H}_2} + N^{\mathrm{H}^-\to\mathrm{H(p)}}_{\mathrm{H(p)/H}^-} R^{\mathrm{H}_2(\nu)\to\mathrm{H}^-}_{\mathrm{H}^-/\mathrm{H}_2}\right]}, \tag{2.4}$$

where the implicit dependencies have been omitted for simplicity.

Due to the dependence of the $R^{\mathrm{H}_2(\nu)\to\mathrm{H}^\star}_{\mathrm{H}^\star/\mathrm{H}_2}$ coefficients on ν, the n_mol estimate obtained from equation (2.4) is affected by the assumptions made on the distribution of the vibrationally excited states of the H_2 molecules. In this work, vibrational excitation of H_2 is addressed by calculating the ν distribution based on the local T_e conditions with the Python tool CRUMPET [19], providing the f_ν factors for equation (2.4). The assumptions and effects of the vibrational excitation are not discussed in this work but will be reported in more detail elsewhere. It is also noted that AMJUEL and H2VIBR provide atomic and molecular data only for H, leaving the validity of the available databases uncertain for studies of molecular processes in D plasmas.

3 Benchmark with synthetic emission

The methods described in section 2 were benchmarked against known references with the help of EDGE2D-EIRENE simulations. The simulations — described in detail in [5] — comprised an L-mode density scan during which the outer divertor ranged from high-recycling to detached conditions, covering a roughly similar space of divertor conditions as the experimental investigations in this work. Utilizing the n_e, T_e, n_at and n_mol outputs of the EDGE2D-EIRENE simulations, the purely atomic D_α, D_γ and D_ε emission components were calculated using the ADAS photon emission coefficients and completed with molecularly induced D_α and D_γ emission calculated by equation (2.3). The total intensities were given as inputs to both the amended optimization presented in this work and the original version presented in [4, 5] without the introduction of $f_{\mathrm{mol},\alpha/\gamma}$ to observe the impact of the unaccounted molecularly induced emission on the solution of the model.

3.1 Reproduction of molecularly induced and purely atomic emission components

The amended model was found to successfully reproduce the molecularly induced fraction of the D_α emission primarily within 25%, as seen in figure 1a. Larger deviations were observed only at $f_{\mathrm{mol},\alpha} < 15\%$, as the estimated $f_{\mathrm{mol},\alpha}$ mostly settles at approximately 10%, heavily overestimating the smallest molecularly induced emission contributions. In accordance with D_α, similar

overestimation is observed for $f_{\mathrm{mol},\gamma}$ which was consistently below 10% in the synthetic investigations. Also the purely atomic emission components were well reproduced with their relative deviations between the emissions calculated from the simulation output and the solutions of the optimization model remaining primarily below 15% in figure 1b. The benchmarks thus suggest good performance of the amended model in distinguishing noticeable molecularly induced emission contributions but strongly compromised accuracy at less significant emission fractions below 10%.

Excluding f_{mol} from the optimization model was expectedly found to lead to overestimation of the purely atomic D_α and D_γ emission components, as the algorithm attempts to reproduce their total emission intensities. For both emission lines, the relative deviations of up to 50–60% are observed in figure 1b between the purely atomic emissions calculated from the simulation output and the solutions of the optimization model, when the increasing fraction of molecularly induced emission is omitted from the optimization. Since the estimation of n_e, T_e and n_at from the intensity ratios relies on the interpretation of the purely atomic emission component via its ADAS representation, ignoring the presence of the molecularly induced emission can be reflected on the estimated plasma conditions. However, due to the tight constraints imposed on n_e and T_e with the help of synthesized line-integrated spectroscopic measurements, this effect was found to be limited to overestimation of n_at, as already postulated in [5].

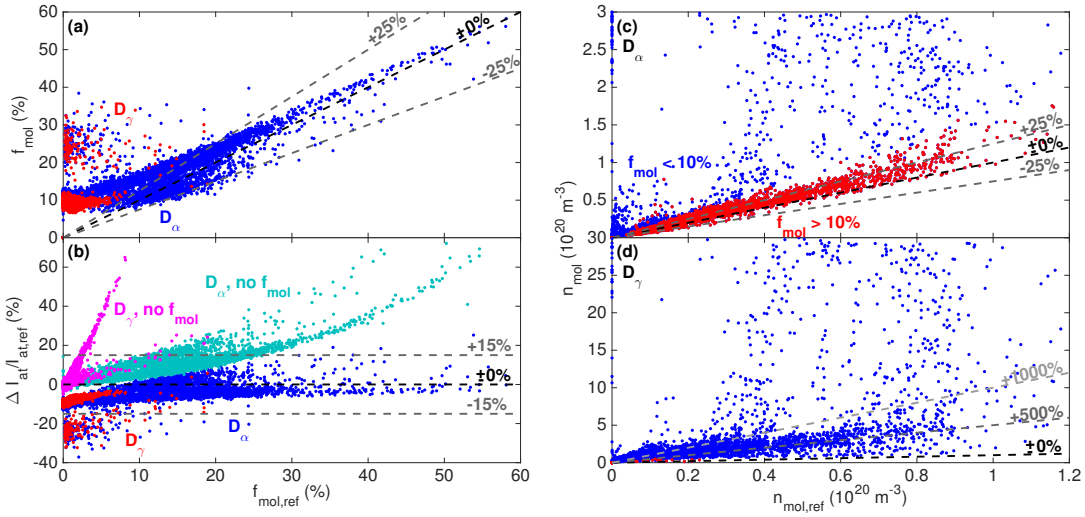

Figure 1. The estimated molecularly induced emission fractions (a) and relative deviations of the estimated purely atomic emission component from the reference (b) as functions of the reference molecularly induced emission fractions calculated from EDGE2D-EIRENE simulation output for D_α (blue) and D_γ (red). The cyan and magenta data points in (b) provide comparison to optimization model without inclusion of f_{mol}. The molecular divertor densities inferred from the estimated molecularly induced D_α (c) and D_γ (d) emission contributions as functions of the reference molecular density from the EDGE2D-EIRENE simulations with molecularly induced emission fractions above (red) and below (blue) 10%.

3.2 Reproduction of molecular divertor density

The divertor n_{mol} was reproduced primarily within 25% of the reference in figure 1c, when equation (2.4) was applied on the solutions of the molecularly induced D_α emission discussed above. Due

to the failure of reproducing molecularly induced emission fractions below 10% in figure 1a, the accuracy of the n_{mol} estimates is lost accordingly, as indicated by the significant scattering of the data in figure 1c for the $f_{\mathrm{mol},\alpha} < 10\%$ cases. Since $f_{\mathrm{mol},\gamma}$ remained consistently below 10% in these benchmarks, no useful n_{mol} estimates were obtained from D_γ, but figure 1d primarily shows overestimation of n_{mol} by a factor of 5–10.

4 Experimental demonstration during detachment in JET L-mode plasmas

The amended methodology was tested experimentally for a JET L-mode density scan, consisting of pulses 94759, 94771 and 94773, during which the outer divertor proceeded from high-recycling conditions to deep detachment. The details of the experiment and the divertor camera analysis of n_{e}, T_{e} and n_{at} made for it have been discussed in [4, 5].

The solutions of the optimization model suggest noticeable contributions of the experimentally distinguished molecularly induced D_α emission near the outer strike point at different stages of detachment, as demonstrated in the example results near the onset of detachment at strike point electron temperature of $T_{\mathrm{e,osp}} \approx 1.4$ eV in figures 2a–c and in deep detachment at $T_{\mathrm{e,osp}} \approx 0.7$ eV in figures 2d–f. In both cases, the effect of the molecularly induced emission is spatially restricted to the vicinity of the divertor target independent of the poloidal extent of the purely atomic component between the outer strike point and the X-point. Near the strike point, the molecularly induced component is observed to significantly amplify the total emission, as well as to slightly widen its distribution radially outwards. The D_γ emission was found to behave qualitatively similarly.

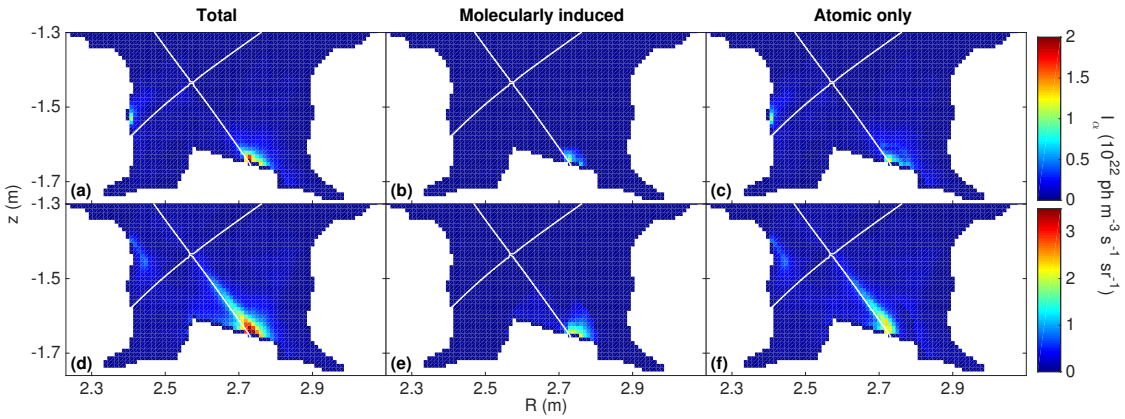

Figure 2. Tomographic reconstructions of the total D_α emission (a,d) and its experimentally distinguished molecularly induced (b,e) and purely atomic (c,f) components at the onset of detachment at $T_{\mathrm{e,osp}} \approx 1.4$ eV (a–c) and in deep detachment at $T_{\mathrm{e,osp}} \approx 0.7$ eV (d–f).

Local investigation at the outer strike point in figure 3b shows the molecularly induced contribution of the D_α emission reaching fractions of up to $f_{\mathrm{mol},\alpha} = 60$–$70\%$ near the onset of detachment at $T_{\mathrm{e,osp}} = 1$–2 eV. When the divertor proceeds to detachment at $T_{\mathrm{e,osp}} < 1.0$ eV — as indicated by the roll-over and decrease of the outer target ion current, Φ_{ot}, in figure 3a — $f_{\mathrm{mol},\alpha}$ is observed to decrease to 10–20%, as the recombination component in equation (2.2) begins to dominate the emission. In high-recycling conditions at $T_{\mathrm{e,osp}} > 2.0$ eV, noticeable fractions of $f_{\mathrm{mo},\alpha} = 40$–$60\%$ are observed, but the estimates have large uncertainties due to the analysis being complicated by

the weaker emission intensities, especially in the case of the recombination-dominated D_ε which is required in the optimization model. The solutions for D_γ show consistently lower molecularly induced fractions mainly at $f_{\mathrm{mol},\gamma}$ = 10–20%, characterized by larger relative uncertainties than for D_α. Based on the benchmark studies discussed in section 3.1, the lowest estimated values at $f_{\mathrm{mol},\gamma} < 10\%$ are to be considered cautiously.

For both D_α and D_γ, the estimated molecularly induced emission fractions in figure 3b lie mostly between the EDGE2D-EIRENE predictions of $f_{\mathrm{mol},\alpha/\gamma}$ obtained using equation 2.3 with the D_2 molecules at their vibrational ground state and with their vibrational distribution calculated by CRUMPET. At $T_{\mathrm{e,osp}} > 2.0$ eV, the modelling predictions show a steep decrease in f_{mol} for both lines with increasing $T_{\mathrm{e,osp}}$ due to a strong increase in the purely atomic emission component from electron-impact excitation, which is not observed experimentally. Without this discrepancy in the behaviour of the purely atomic emission, closer agreement in the molecularly induced fraction would likely be achieved. Considering the otherwise good agreement between the experiment and the modelling — especially as the experimental f_{mol} estimates are freely ranging variables in the optimization model with no connection to the physical presentations behind equation 2.3 — the observations suggest promising prospects for the amended analysis method to experimentally distinguish the molecularly induced emission components.

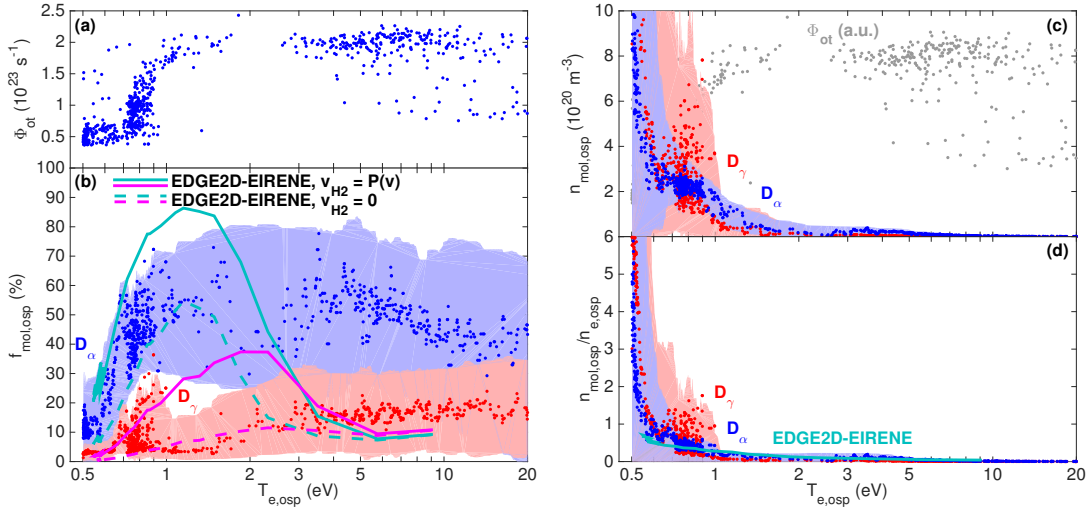

Figure 3. Roll-over of the outer target ion current, Φ_{ot}, (a) to detachment as a function of the outer strike point electron temperature. Experimental estimates (data points) and EDGE2D-EIRENE predictions (lines) of the molecularly induced emission fraction (b) of D_α (blue, cyan) and D_γ (red, magenta) at the outer strike point. The modelling references are presented with (solid) and without (dashed) consideration of the vibrational excitation of the D_2 molecules. Molecular density (c) and its ratio to local electron density (d) at the outer strike point inferred from the experimentally distinguished molecularly induced D_α (blue) and D_γ (red) emissions as functions of $T_{\mathrm{e,osp}}$ with comparison to EDGE2D-EIRENE predictions (d, cyan). The shaded blue and red regions in (b–d) represent the uncertainties of the experimental estimates, and the gray data points in (c) demonstrate the roll-over of Φ_{ot} in arbitrary units as guidance of the detachment process. Note the logarithmic $T_{\mathrm{e,osp}}$ axes.

The molecular density inferred from the molecularly induced D_α emission at the outer strike point was observed to increase with decreasing $T_{\mathrm{e,osp}}$ at $T_{\mathrm{e,osp}} < 2.0$ eV up to approximately $n_{\mathrm{mol}} \approx$

3×10^{20} m^{-3} in deep detachment at $T_{e,osp} = 0.7$ eV, as presented in figure 3c. Below $T_{e,osp} = 0.7$ eV, the observed steep increase to the order of 10^{21} m^{-3} is characterized by large uncertainties due to $f_{mol,\alpha}$ falling to low values of approximately 10% in figure 3b. The n_{mol} estimate inferred from $f_{mol,\gamma}$ lies mostly within the error bars of n_{mol} given by $f_{mol,\alpha}$, albeit with significantly increased uncertainties already at $T_{e,osp} < 1.0$ eV due to the consistently lower molecularly induced emission fraction of D_γ. The close agreement between the independent n_{mol} estimates inferred from the two emission lines is a positive demonstration of the functionality of the method. Due to noticeably different levels of the divertor n_e between the experimental estimates and the EDGE2D-EIRENE predictions — as described in detail in [5] — direct comparison of n_{mol} was not found feasible. As an indicative comparison, however, both analyses agree within scatter of the experimental data on n_{mol} reaching 50–100% of the local n_e at the outer strike point in figure 3c.

Unlike the solutions for $f_{mol,\alpha/\gamma}$, the inferred n_{mol} estimates are strongly dependent on the assumptions made for the vibrational excitation of the D_2 molecules. The experimental n_{mol} estimates presented in figures 3c and d were obtained by calculating the distribution of the vibrationally excited states of the D_2 molecules for equation (2.4) by CRUMPET with the help of the local estimates for the divertor T_e. Ignoring the vibrational excitation and using AMJUEL and H2VIBR rates for the vibrational ground state only increased the inferred n_{mol} estimates approximately by a factor of five, severely degrading the agreement on the $\frac{n_{mol}}{n_e}$ ratio between the experimental estimates and the EDGE2D-EIRENE predictions. The strong effect of the assumptions of the vibrational states of the molecules indicates need for improved knowledge on the distribution of the vibrational excitation states for increased reliability of the method.

5 Conclusions

Previously presented methodology for estimating divertor plasma conditions in JET from intensity ratios of camera observations of the deuterium Balmer lines has been amended to distinguish the purely atomic and molecularly induced emission components from the total emission intensity. With the help of the molecular databases of EIRENE, the separated molecularly induced emission contribution can be used to infer estimates for the molecular divertor density.

The amended method was benchmarked using synthetic emission data from EDGE2D-EIRENE simulations and found to reproduce the molecularly induced emission within 25% of the reference, when molecular processes accounted for more than 10% of the total emission. Similar accuracy was achieved also in reproducing the divertor n_{mol}.

Experimental analysis of a JET L-mode density scan suggested molecularly induced contributions of up to 60–70% at the outer strike point for the D_α emission at the onset of detachment with decrease to 10–20% in deep detachment due to increasing dominance of atomic recombination. For D_γ, significantly lower contributions mainly below 20% were observed. The experimentally estimated molecularly induced emission fractions mostly agreed with those calculated from the EDGE2D-EIRENE simulation outputs within the variation range set by different assumptions of vibrational excitation of the D_2 molecules. The n_{mol} estimates inferred from the molecularly induced D_α and D_γ contributions independently from each other agreed within uncertainties, showing increase of n_{mol} at the outer strike point in detachment with decreasing $T_{e,osp}$ up to $n_{mol} \approx 3 \times 10^{20}$

m^{-3} in deep detachment at $T_{e,osp} = 0.7$ eV with matching $\frac{n_{mol}}{n_e}$ ratio with the EDGE2D-EIRENE predictions within the scatter of the experimental data.

Due to the dependence of the applied molecular data on the vibrational excitation of the molecules, the inference of n_{mol} from the experimentally distinguished molecularly induced emission components is strongly affected by the assumptions made on the population distribution of the vibrationally excited states. Moreover, the molecular data exists only for H_2, while the majority of JET plasma experiments are conducted with D. Deeper understanding of the vibrational excitation of the D_2 molecules and the effect of the fuel isotope on the molecular processes resulting in Balmer line emission are thus required for improved accuracy of the method.

Acknowledgments

This work has been carried out within the framework of the EUROfusion Consortium and has received funding from the Euratom research and training programme 2014-2018 and 2019-2020 under grant agreement No 633053. The views and opinions expressed herein do not necessarily reflect those of the European Commission.

References

[1] D. Wünderlich et al., Atoms **4** (2016) 26
[2] K. Verhaegh et al., Plasma Physics and Controlled Fusion **63** (2021) 035018
[3] B. Lomanowski et al., 23rd International Conference on Plasma Surface Interactions in Controlled Fusion Devices (2018)
[4] J. Karhunen et al., Nuclear Materials and Energy **25** (2020) 100831
[5] J. Karhunen et al., Plasma Physics and Controlled Fusion **63** (2021) 085018
[6] R. Simonini et al., Contributions to Plasma Physics **34** (1997) 368
[7] D. Reiter et al., Journal of Nuclear Materials **196–198** (1992) 80–89
[8] S. Wiesen, "EDGE2D/EIRENE code interface report", JET ITC-Report (2006)
[9] A. Huber et al., Journal of Nuclear Materials **313–316** (2003) 925–930
[10] A. Huber et al., Review of Scientific Instruments **83** (2012) 10D511
[11] J.R. Harrison et al., Journal of Nuclear Materials **415** (2011) S379–S382
[12] J. Karhunen et al., Review of Scientific Instruments **90** (2019) 103504
[13] W.K. Hastings et al., Biometrika **57** (1970) 97–109
[14] A. Patil et al., Journal of Statistical Software **35** (2010) 1–81
[15] H.P. Summers, "The ADAS user manual", version 2.6 (2004), available at `www.adas.ac.uk`
[16] A.G. Meigs et al., 27th EPS Conference on Plasma Physics (2000)
[17] B. Lomanowski et al., Nuclear Fusion **55** (2015) 123028
[18] B. Lomanowski et al., Plasma Physics and Controlled Fusion **62** (2020) 065006
[19] A. Holm et al., Nuclear Materials and Energy **27** (2021) 100982